








ARTICLE

Inhibiting antibiotic-resistant Enterobacteriaceae by microbiota-mediated intracellular acidification

Matthew T. Sorbara^{1,3}, Krista Dubin^{1,7}, Eric R. Littmann³, Thomas U. Moody^{1,3}, Emily Fontana³ , Ruth Seok^{1,3} , Ingrid M. Leiner^{1,2,3} , Ying Taur^{2,7}, Jonathan U. Peled^{4,7} , Marcel R.M. van den Brink^{4,7} , Yael Litvak⁵ , Andreas J. Bäuml⁵, Jean-Luc Chaubard⁶, Amanda J. Pickard⁶, Justin R. Cross⁶, and Eric G. Pamer^{1,2,3,7} 

***Klebsiella pneumoniae*, *Escherichia coli*, and other members of the Enterobacteriaceae family are common human pathogens that have acquired broad antibiotic resistance, rendering infection by some strains virtually untreatable. Enterobacteriaceae are intestinal residents, but generally represent <1% of the adult colonic microbiota. Antibiotic-mediated destruction of the microbiota enables Enterobacteriaceae to expand to high densities in the colon, markedly increasing the risk of bloodstream invasion, sepsis, and death. Here, we demonstrate that an antibiotic-naive microbiota suppresses growth of antibiotic-resistant clinical isolates of *Klebsiella pneumoniae*, *Escherichia coli*, and *Proteus mirabilis* by acidifying the proximal colon and triggering short chain fatty acid (SCFA)-mediated intracellular acidification. High concentrations of SCFAs and the acidic environment counter the competitive edge that O₂ and NO₃ respiration confer upon Enterobacteriaceae during expansion. Reestablishment of a microbiota that produces SCFAs enhances clearance of *Klebsiella pneumoniae*, *Escherichia coli*, and *Proteus mirabilis* from the intestinal lumen and represents a potential therapeutic approach to enhance clearance of antibiotic-resistant pathogens.**

Introduction

One of the critical functions of a healthy intestinal microbiota is to provide colonization resistance against a variety of bona fide and potential pathogens. Anaerobic bacteria in the Firmicutes and Bacteroidetes phyla are the dominant constituents of the normal colonic microbiota and together can provide colonization resistance through both direct (bacteria-bacteria) and indirect (host mediated) mechanisms (Human Microbiome Project Consortium, 2012; Buffie and Pamer, 2013). Several mechanisms of colonization resistance against intestinal pathogens have been described, including competition for nutrients (Kamada et al., 2012), short chain fatty acid (SCFA)-dependent inhibition of virulence and replication (Bohnhoff et al., 1964a,b; Lawhon et al., 2002; Gantois et al., 2006), and direct antagonism through bacteriocin production or Type VI Secretion System-mediated killing (Rea et al., 2010; Hecht et al., 2016). In addition, some pathogens use strategies to counter or evade these mechanisms of colonization resistance (Sorbara and Pamer, 2018). Therefore, the ability of a particular pathogenic strain to expand in the intestine will be determined by both the characteristics of the host microbiota's colonization resistance and the invading strain's ability to counter that resistance.

ota's colonization resistance and the invading strain's ability to counter that resistance.

The microbiota's capacity to provide colonization resistance is essential for protection from enteric pathogens, including food-borne pathogens such as *Salmonella enterica* serovar Typhimurium (*S. Typhimurium*), *Campylobacter jejuni*, and *Listeria monocytogenes* (Bohnhoff et al., 1964a; O'Loughlin et al., 2015; Becattini et al., 2017). Expansion of these pathogens in the gastrointestinal tract drives inflammatory responses and gastroenteritis. In some cases, the induction of inflammatory responses in the host provides these pathogens with a competitive advantage and enables their rapid expansion (Lupp et al., 2007). For example, during infection with pathogenic *S. Typhimurium* or *Escherichia coli*, inflammation and disruption of the microbiota leads to increased availability of oxygen and nitrates in the lumen, which can be used by respiration-competent pathogens as terminal electron acceptors in electron transport chains (Winter et al., 2013; Byndloss et al., 2017).

In healthcare settings, antibiotic-mediated disruption of the microbiota can be associated with enteric expansion of members

¹Immunology Program, Sloan Kettering Institute, Memorial Sloan Kettering Cancer Center, New York, NY; ²Infectious Diseases Service, Department of Medicine, Memorial Sloan Kettering Cancer Center, New York, NY; ³Center for Microbes, Inflammation and Cancer, Memorial Sloan Kettering Cancer Center, New York, NY; ⁴Adult Bone Marrow Transplant Service, Department of Medicine, Memorial Sloan Kettering Cancer Center, New York, NY; ⁵Department of Medical Microbiology and Immunology, University of California, Davis School of Medicine, Davis, CA; ⁶Donald B. and Catherine C. Marron Cancer Metabolism Center, Sloan Kettering Institute, Memorial Sloan Kettering Cancer Center, New York, NY; ⁷Weill Cornell Medical College, New York, NY.

Correspondence to Eric G. Pamer: pamere@mskcc.org; Matthew T. Sorbara: sorbaram@mskcc.org.

© 2018 Sorbara et al. This article is distributed under the terms of an Attribution-Noncommercial-Share Alike-No Mirror Sites license for the first six months after the publication date (see <http://www.rupress.org/terms/>). After six months it is available under a Creative Commons License (Attribution-Noncommercial-Share Alike 4.0 International license, as described at <https://creativecommons.org/licenses/by-nc-sa/4.0/>).

of the Enterobacteriaceae family, including *E. coli* and *Klebsiella pneumoniae*, as well as vancomycin-resistant *Enterococci* and *Clostridium difficile* (Kim et al., 2017). While *C. difficile* causes gastroenteritis, hospital-associated Enterobacteriaceae and vancomycin-resistant *Enterococci* strains often expand in the gut without triggering overt inflammatory responses. In these instances, the primary clinical concern is that expansion of these species in the gut increases the risk for subsequent development of a bloodstream infection (BSI) in vulnerable patient populations. For example, allogeneic hematopoietic stem cell transplantation (allo-HCT) is an effective but highly immunocompromising treatment for some forms of cancer. The high incidence and risk of bacterial infections in patients undergoing allo-HCT necessitates administration of prophylactic and empiric antibiotics, leading to destruction of the normal microbiome. In this patient population, enteric domination with Enterobacteriaceae leads to a significant increase in the risk of developing a BSI (Taur et al., 2012). Furthermore, an increasing proportion of clinical isolates of Enterobacteriaceae are resistant to a wide range of antibiotics, including strains that produce extended-spectrum- β -lactamases or carbapenemases (Centers for Disease Control and Prevention, 2013). Accordingly, BSI with these highly antibiotic-resistant strains are increasingly challenging to treat.

The observation that antibiotic-mediated destruction of the microbiota is associated with expansion of Enterobacteriaceae (van der Waaij et al., 1971) suggests that the healthy microbiota has the capacity to prevent the expansion of these strains. Although colitis enhances expansion of Enterobacteriaceae in the gut (Lupp et al., 2007), enteric expansion of highly antibiotic-resistant Enterobacteriaceae often occurs in the absence of colitis and thus most likely results from the inactivation of microbiota-mediated inhibitory mechanisms that remain incompletely defined. In this study, we demonstrate that the microbiota can provide effective direct colonization resistance against antibiotic-resistant clinical isolates of *K. pneumoniae*, *E. coli*, and *Proteus mirabilis* and identified the major mechanism of that resistance. Surprisingly, the inhibition of Enterobacteriaceae is completely dependent on an acidified pH. Coupled with the production of high levels of SCFA, this acidified environment triggers intracellular acidification of Enterobacteriaceae to levels that prevent replication. Furthermore, SCFA-mediated inhibition prevents the utilization of respiration as a mechanism for competitive advantage during Enterobacteriaceae expansion. Finally, we demonstrate in a patient undergoing allo-HCT that a decrease in SCFA levels correlates with enteric expansion of *E. coli* leading to development of a BSI.

Results

The microbiota provides colonization resistance and colonization clearance against antibiotic-resistant Enterobacteriaceae

To directly investigate whether the microbiota provides resistance against antibiotic-resistant clinical isolates of Enterobacteriaceae, we used two isolates each of *K. pneumoniae*, *E. coli*, and *P. mirabilis*. All six strains were resistant to ampicillin, in addition to other antibiotics (Table S1; Xiong et al., 2015). In par-

ticular, two strains, *K. pneumoniae* MH258 and *E. coli* MHX43, are carbapenemase and extended-spectrum- β -lactamase expressing, respectively, and thus represent the emerging group of highly antibiotic-resistant strains. Mice were treated with ampicillin in their drinking water to disrupt the microbiota and were challenged with the clinical isolates (Fig. 1 A). All isolates expanded to high levels in antibiotic-treated mice, but failed to expand in control mice (Fig. 1 A). Similarly, *K. pneumoniae* MH258 rapidly expanded to high levels in the gut of un-reconstituted gnotobiotic mice, but did not expand in mice reconstituted with a diverse microbiota from a naive mouse (Fig. 1 B and Fig. S1 A). These results demonstrate that the microbiota provides high levels of colonization resistance against these antibiotic-resistant Enterobacteriaceae isolates.

We next asked if administration of an antibiotic-naive microbiota can mediate colonization clearance of Enterobacteriaceae. We colonized antibiotic-treated mice with *K. pneumoniae*, *E. coli*, or *P. mirabilis* and then administered a fecal microbiota transplant (FMT) from antibiotic-naive WT mice (Fig. 1, C–E). FMT treatments significantly reduced colonization with *K. pneumoniae*, *E. coli*, and *P. mirabilis* compared with PBS-treated mice (Fig. 1, C–E). Some PBS-treated control mice also partially reduced Enterobacteriaceae colonization density over the course of 2 wk, suggesting that there is partial recovery of colonization resistance. In support of this notion, microbiota composition partially recovered in PBS-treated mice toward the composition of naive mice, while FMT treatment led to a return to a configuration that was indistinguishable from the naive state by PCA analysis (Fig. S1 B).

Inhibition of carbapenem-resistant *K. pneumoniae* is pH dependent

To determine the primary mechanism by which the microbiota prevents expansion and enhances clearance of these antibiotic-resistant isolates, we first tested whether the microbiota directly stops growth or whether inhibition was dependent on an indirect, host-mediated function. To distinguish between these possibilities, we inoculated cultured cecal contents from antibiotic-naive or antibiotic-treated mice with *K. pneumoniae* under anaerobic conditions (Fig. 2 A). While *K. pneumoniae* expanded to high densities in cecal contents from antibiotic-treated mice, cecal contents obtained from antibiotic-naive mice did not support *K. pneumoniae* growth, consistent with a direct role of the microbiota in preventing expansion (Fig. 2 B). Type VI Secretion Systems have been identified as mediators of antagonism between Gram-negative species through contact-dependent mechanisms (Russell et al., 2014). To determine whether inhibition of *K. pneumoniae* by cecal contents from antibiotic-naive mice requires direct contact with commensal bacteria, we cultured *K. pneumoniae* in filtered cecal contents and found that inhibition was intact (Fig. 2 C). Importantly, we found that the same pattern of inhibition and expansion was consistent for the other clinical isolates we tested (Fig. S2). Therefore, the microbiota is capable of directly preventing the replication of these antibiotic-resistant Enterobacteriaceae in a manner that is contact independent.

In some contexts, the microbiota is able to limit pathogen replication by limiting nutrient availability (Kamada et al., 2012; Ng

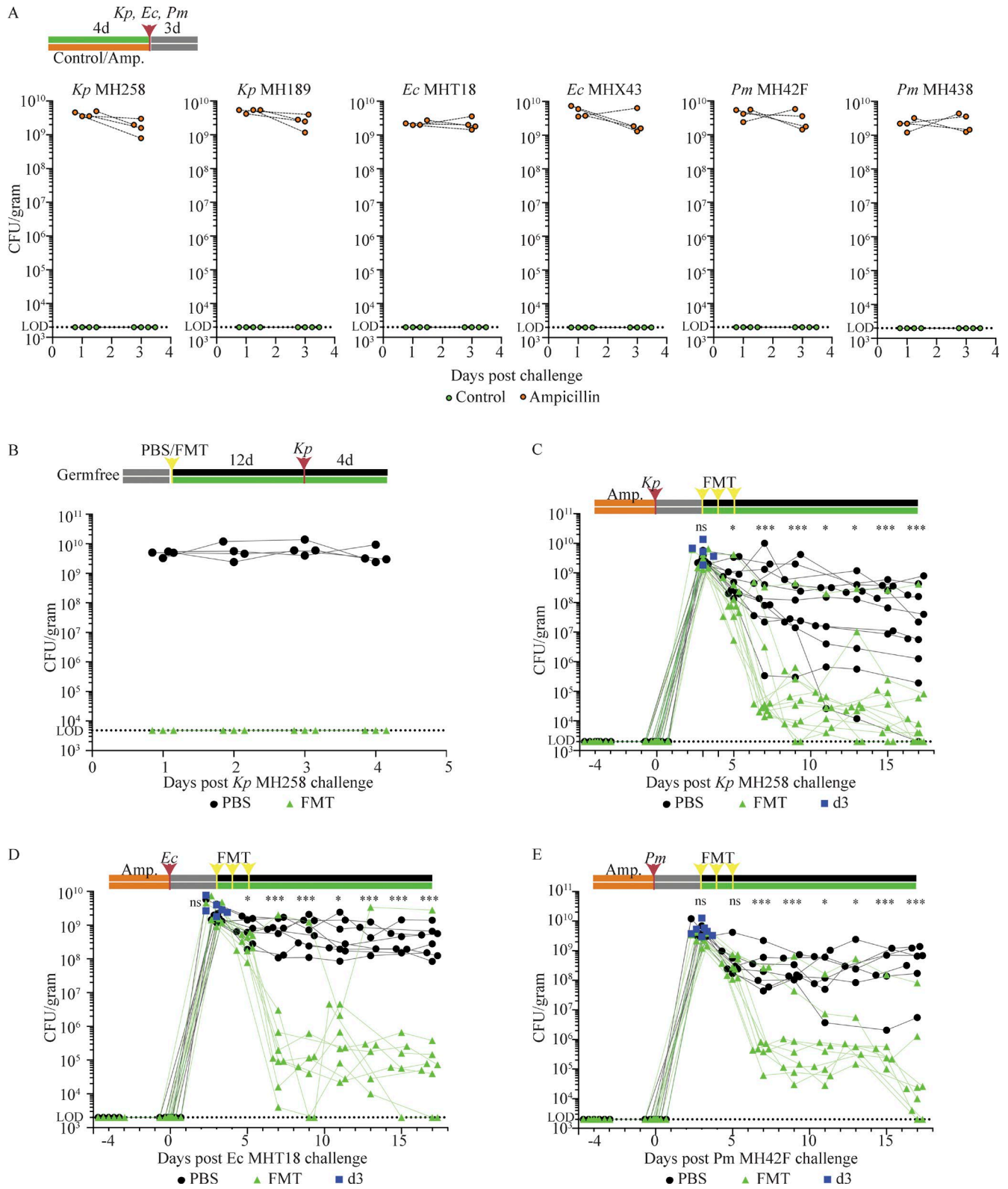


Figure 1. **A diverse microbiota blocks enteric expansion and promotes clearance of clinical Enterobacteriaceae isolates.** (A) Antibiotic-naive or ampicillin-treated WT mice were challenged with the indicated isolates of Enterobacteriaceae, and colonization after 24 and 72 h was measured by measuring CFUs in fecal pellets ($n = 4$ mice from two experiments). (B) Colonization of *K. pneumoniae* MH258 in fecal samples 1–4 d after challenge in gnotobiotic mice reconstituted with an antibiotic-naive microbiota or PBS as indicated in the schematic diagram ($n = 3, 4$ mice from one representative experiment of two independent experiments). (C–E) Colonization with *K. pneumoniae* MH258 (C), *E. coli* MHT18 (D), or *P. mirabilis* MH42F (E) in fecal pellets from ampicillin-treated WT mice that were challenged with *K. pneumoniae* MH258, *E. coli* MHT18, or *P. mirabilis* MH42F and then given FMT or PBS treatments as indicated. ($n = 7$ –12 mice per group from three to four independent experiments; t test with the Holm-Sidak method to correct for multiple comparisons was used to compare the PBS and FMT groups at each time point). *, $P < 0.05$; ***, $P < 0.001$. ns, not significant.

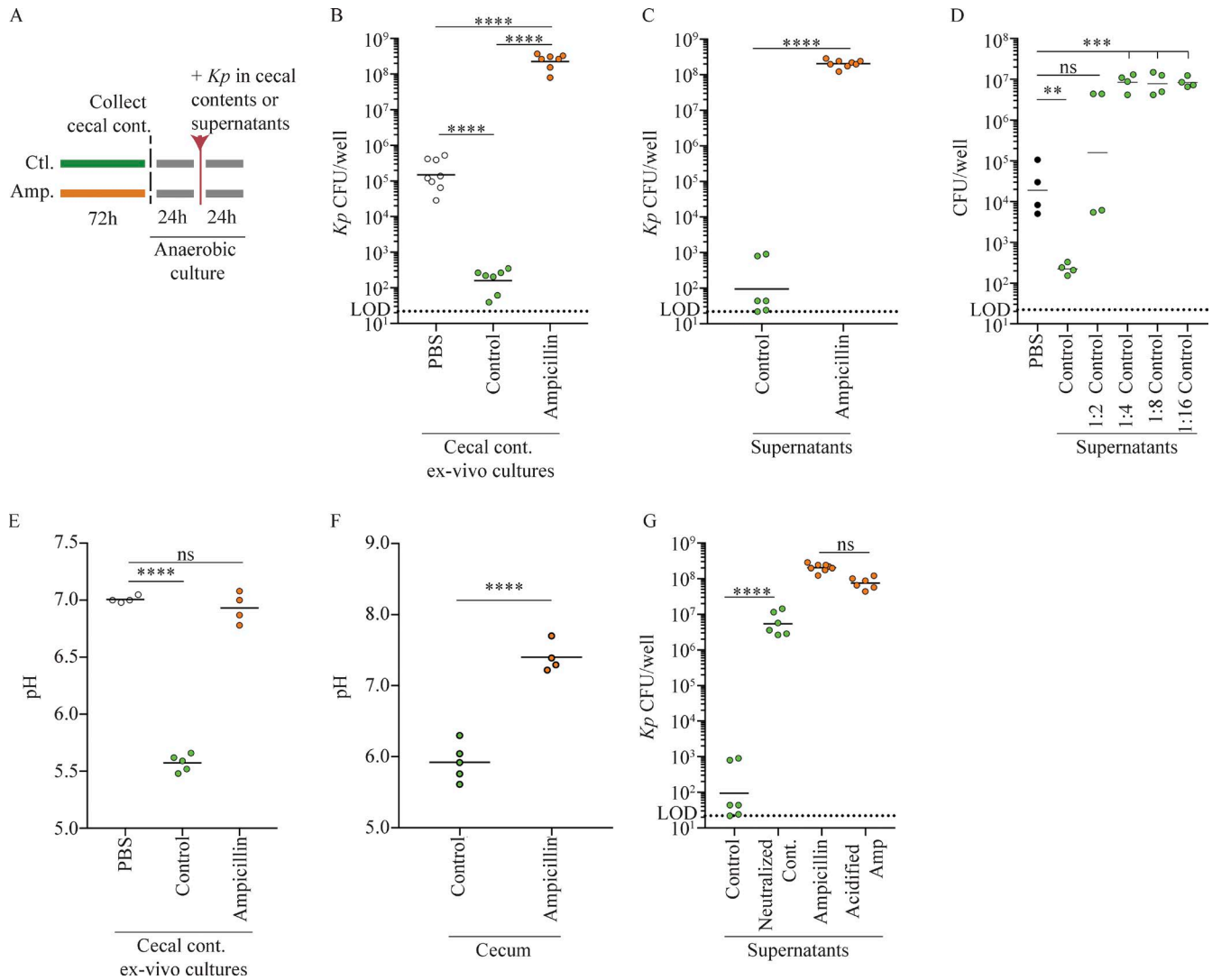


Figure 2. An acidified pH is necessary for the microbiota to directly block carbapenem resistant *K. pneumoniae* expansion. (A) Schematic showing the collection and anaerobic culture of cecal contents from antibiotic-naive or ampicillin-treated mice. (B) Growth of *K. pneumoniae* MH258 in cecal content cultures from antibiotic-treated or antibiotic-naive mice ($n = 7-8$ wells from three to four independent experiments; one-way ANOVA followed by Dunnett's multiple comparison test to PBS control values). (C) Growth of *K. pneumoniae* MH258 in the supernatant from the indicated cecal content supernatants ($n = 6-8$ wells from three independent experiments; t test). Data from these conditions is also presented in G. (D) Growth of *K. pneumoniae* MH258 in diluted supernatants from cultures of antibiotic-naive mice ($n = 4$ wells from two independent experiments; one-way ANOVA followed by Dunnett's multiple comparison test to the PBS control values). (E) pH of supernatants from the indicated cecal content cultures ($n = 4-5$ independent experiments; one-way ANOVA followed by Dunnett's multiple comparison test to the PBS control values). (F) pH of freshly isolated cecal contents from antibiotic-naive or ampicillin-treated mice ($n = 4-5$ independent experiments; t test). (G) Growth of *K. pneumoniae* MH258 in the supernatant from the indicated cecal content cultures, with or without adjusting the pH as indicated ($n = 6-8$ wells from three independent experiments, one-way ANOVA followed by Sidak's Multiple comparison test). Control conditions without pH adjustment are also presented in C. *, $P < 0.05$; **, $P < 0.01$; ***, $P < 0.001$. *Kp*, *K. pneumoniae*.

et al., 2013). To distinguish between nutrient limitation and the production of inhibitory factors as mediators of growth suppression in the context of these clinical isolates, we serially diluted antibiotic-naive cecal content supernatant with PBS. Diluted cecal content supernatant supported expansion of *K. pneumoniae* to levels higher than the PBS control (Fig. 2 D), indicating that production of an inhibitory factor, not nutrient limitation, suppresses expansion of *K. pneumoniae*.

Next, we observed that culture of antibiotic-naive cecal contents, but not ampicillin-treated contents, led to acidification relative to the PBS control (Fig. 2 E). To determine if a similar change in pH occurred in vivo, we measured the pH of directly

isolated cecal contents from antibiotic-naive mice and found that the cecal pH was 1.47 units lower than cecal contents from ampicillin-treated mice (Fig. 2 F). The measured cecal pH of 5.94 is similar to that reported in human studies measuring pH in the gastrointestinal tract (Farmer et al., 2014). Surprisingly, neutralization with NaOH enabled a 4–5 log increase in *K. pneumoniae* growth in cecal content supernatants from antibiotic-naive mice, demonstrating that acid pH is necessary to prevent *K. pneumoniae* expansion (Fig. 2 G). However, acid pH alone is not sufficient to prevent *K. pneumoniae* growth, since acidification with HCl of cecal content supernatant from antibiotic-treated mice did not prevent *K. pneumoniae* expansion (Fig. 2 G). These results

demonstrate that acid pH in cecal contents is necessary but not sufficient to prevent *K. pneumoniae* expansion.

Physiological concentrations of SCFAs inhibit Enterobacteriaceae

In the anaerobic environment of the healthy lower gastrointestinal tract, the microbiota breaks down dietary fiber to monosaccharides, which, upon fermentation, lead to release of large quantities of SCFAs as by-products (Topping and Clifton, 2001). Loss of SCFA has been associated with loss of colonization resistance against *S. Typhimurium*, an enteric pathogen that invades intestinal epithelial cells leading to intense inflammatory responses (Bohnhoff et al., 1964a,b; Jacobson et al., 2018). However, SCFA production can be influenced both by diet and microbiota composition (Sonnenburg and Sonnenburg, 2014). Therefore, we measured the concentration of SCFA in mice from our animal facility. In antibiotic-naïve mice, acetate, propionate, and butyrate production by the microbiota lead to steady-state total concentrations of these SCFA in excess of 80 mM in the cecum (Fig. 3 A). Antibiotic treatment markedly reduced SCFA concentrations (Fig. 3 A). Next, we asked whether these physiological concentrations of SCFAs inhibit expansion of the antibiotic-resistant *E. coli*, *K. pneumoniae*, and *P. mirabilis* isolates. Therefore, we tested the impact of a physiological mixture of SCFA at neutral (7.0) and acidic (5.75) pH on *K. pneumoniae*, *E. coli*, and *P. mirabilis* growth (Fig. 3 B). While all strains grew well at pH 5.75 in the absence of SCFA and were not inhibited by SCFA at pH 7.0, they were significantly inhibited by the presence of physiological concentrations of SCFAs at pH 5.75 (Fig. 3 B). Furthermore, physiological concentrations of SCFAs inhibited the growth of the Enterobacteriaceae isolates across the pH range observed in cecal contents from antibiotic naïve mice (Fig. 3 C). In addition, we observed strain-specific variation in the extent of growth inhibition at acidified pH values, with *E. coli* MHX43 and *P. mirabilis* MH42F being more strongly inhibited at pH of 5.75 or 6.00 (Fig. 3 C). These results indicate that cecal concentrations of SCFA suppress Enterobacteriaceae growth in a pH-dependent fashion.

We next asked if variations in the rescue of in vivo SCFA production could explain the variations in clearance of the clinical isolates we observed following PBS or FMT treatment (Fig. 1, C–E). To address this, we measured acetate, propionate, and butyrate levels in the cecum of these *K. pneumoniae*-, *E. coli*-, and *P. mirabilis*-colonized mice. First, we asked if these strains themselves contributed to high SCFA levels in vivo, since *E. coli* can produce acetate under in vitro conditions (Luli and Strohl, 1990). During the initial peak of Enterobacteriaceae domination before treatment (day 3), cecal SCFA concentrations remained low (Fig. 3 D, blue symbols; and Fig. S3), indicating that *K. pneumoniae*, *E. coli*, or *P. mirabilis* do produce sufficient acetate in vivo to lead to accumulation. Therapeutic reintroduction of the microbiota increased SCFA levels, and there was a partial recovery in PBS-treated mice compared with this day 3 time point (Fig. S3). Strikingly, there was a significant correlation ($P < 0.0001$) between the total level of SCFA production and the decrease in *K. pneumoniae*, *E. coli*, and *P. mirabilis* colonization across both PBS- and FMT-treated mice (Fig. 3 D).

An acidic pH and SCFAs reduce the advantage Enterobacteriaceae gain through respiration

Recent studies have demonstrated that the ability of Enterobacteriaceae to respire is critical for optimal expansion in an inflamed or dysbiotic gut and that strains that can use oxygen or nitrate as terminal electron acceptors outcompete deficient strains in the inflamed gut (Winter et al., 2013; Byndloss et al., 2017). It is unclear, however, whether the presence of terminal electron acceptors allows Enterobacteriaceae to overcome SCFA-mediated inhibition and whether SCFAs and pH impact the growth advantages conferred by ability to use O_2 or NO_3 . To test this, we used an assay in which WT *E. coli* were grown in competition with a mutant strain that is unable to use microaerophilic concentrations of O_2 or NO_3 as terminal electron acceptors. Both the total growth of *E. coli* and the relative advantage of the WT compared with mutant were measured under conditions with or without acidic pH, oxygen, nitrates, and a physiological mixture of SCFA (Fig. 4 A).

The advantage of WT over mutant *E. coli* (competitive index; CI) increased with the addition of oxygen or nitrates, and was highest in conditions most closely resembling antibiotic-treated mice (+ O_2 , + NO_3 , -SCFA, high pH; Fig. 4 B and Table S2), which is consistent with earlier reports demonstrating a strong competitive advantage for respiration-competent strains under these conditions (Winter et al., 2013; Byndloss et al., 2017). In contrast, in conditions resembling antibiotic naïve mice (- O_2 , - NO_3 , +SCFA, acidified pH), the relative advantage of respiration was $\sim 7,500\times$ lower (Fig. 4 B and Table S2). Surprisingly, acidifying the culture media, even in the absence of SCFA, led to a reduced CI across conditions (Fig. 4 B and Table S2). Growth of the respiration-incompetent strain was impacted more by pH than either oxygen or nitrate concentrations in paired conditions (Table S2). Despite these significant changes in the competitive advantage gained by respiration, only addition of SCFA at an acidic pH reduced total replication of *E. coli* independent of oxygen or nitrate status (Fig. 4 B). We next sought to confirm that these effects also occurred when *E. coli* were growing on the nutrients present in the gut. Therefore, we performed experiments to determine the relationship between oxygen/SCFA/pH and both total *E. coli* growth and respiration advantage in supernatants of cecal content cultures from antibiotic-naïve or antibiotic-treated mice (Fig. S4 and Table S2). Similar to our findings in Luria-Bertani (LB) broth, anaerobic growth and acidic pH both reduced the competitive advantage gained through respiration. In this system, addition of NO_3 had a minor impact on the CI in paired conditions (data not shown). The presence of SCFAs at an acidic pH, either produced naturally by the microbiota (antibiotic naïve) or directly added (antibiotic-treated conditions), was necessary to reduce *E. coli* replication. These experiments indicate that loss of SCFAs leads to Enterobacteriaceae domination, and in the setting of increased pH, bacterial strains that can use O_2 or NO_3 to respire have a competitive advantage.

SCFA mediate intracellular acidification of antibiotic resistant *K. pneumoniae* and *E. coli*

We next investigated the mechanism by which SCFA directly inhibit these isolates. SCFA are weak acids that become membrane permeable as they become protonated at lower pH, and intracellu-

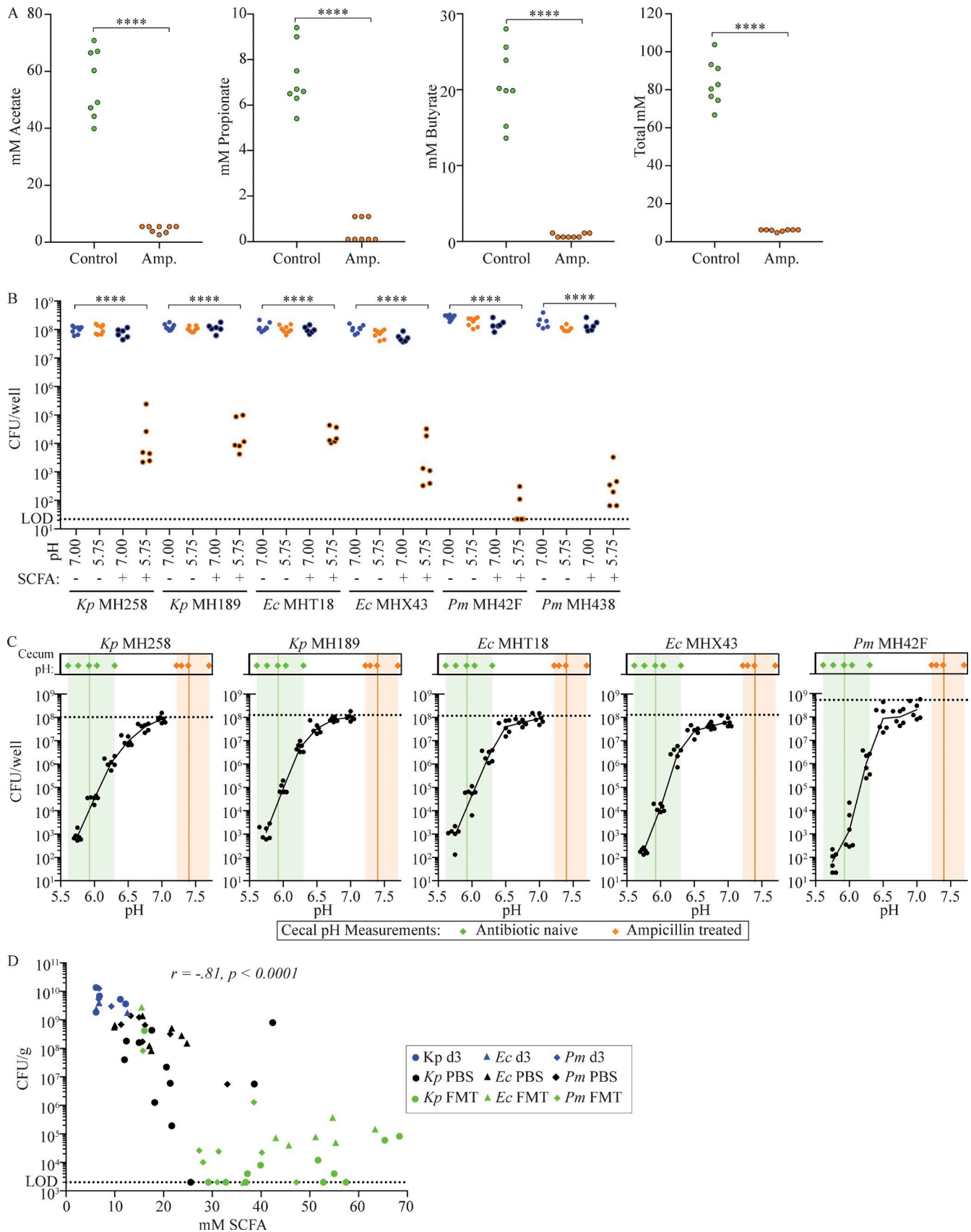


Figure 3. **SCFAs inhibit Enterobacteriaceae isolates.** (A) Acetate, propionate, and butyrate concentrations in antibiotic-naive or ampicillin mice. Total SCFA represents the sum of these three most-abundant SCFA ($n = 8$ mice from two independent experiments; t test). (B) Growth of the indicated isolates of Enterobacteriaceae in LB with or without a mixture of SCFA at the indicated pH was measured after 16 h of incubation ($n = 6-8$ wells from three to four independent

lar proton release in bacteria has been shown to disrupt pH homeostasis (Salmond et al., 1984; Roe et al., 1998). Therefore, we asked if physiological concentrations of SCFA are sufficient to drive intracellular acidification in these antibiotic-resistant isolates using a GFP-reporter assay that we adapted for use by flow cytometry (Martinez et al., 2012). We generated *K. pneumoniae* MH258 and *E. coli* MHT18 strains expressing a pH-sensitive GFP and equilibrated the intracellular and extracellular pH to generate standard curves for intracellular pH (Fig. 5 A). As expected, *E. coli* and *K. pneumoniae* maintained a slightly alkaline intracellular pH, which was not disrupted by an environmental shift to an acidic pH in the absence of SCFA (Fig. 5, B and C). However, addition of physiological concentrations of acetate led to intracellular acidification and a decrease in the Δ pH compared with the extracellular environment (Fig. 5, B and C). Increasing concentrations of propionate and butyrate also triggered intracellular acidification (Fig. S5). However, while physiological concentrations (>10 mM) of butyrate are sufficient to trigger moderate acidification (Fig. S5), propionate did not trigger acidification at the measured cecal concentrations (<10 mM; Fig. 3 A and Fig. S5). Therefore, as a result of the ratio of acetate/propionate/butyrate observed in our facility, as well as in human studies (den Besten et al., 2013), acetate is likely the primary driver of intracellular acidification under physiological conditions. We next performed the assay in freshly isolated cecal contents to determine if other soluble components in this more complex environment would prevent SCFA-mediated acidification. Freshly isolated WT mouse cecal contents led to intracellular acidification to pH 6.25 of *K. pneumoniae* at slightly acidic but not neutral external pH, indicating that natural concentrations of SCFA are sufficient to drive this response (Fig. 5 D). Furthermore, extracellular acidification did not lead to consistent acidification in cecal contents from ampicillin-treated mice (Fig. 5 D). In line with a central role for acetate, intracellular acidification could be rescued by addition of a physiological concentration of acetate alone (Fig. 5 D). We next sought to determine what internal pH was necessary for *K. pneumoniae* and *E. coli* replication by titrating the pH in conditions where the external and internal pH were equalized. Decreasing internal pH values starting from pH 8.25 resulted in stepwise decreases in *E. coli* and *K. pneumoniae* replication rates (Fig. 5 E). *K. pneumoniae* and *E. coli* failed to replicate above input levels at internal pHs of 7.25 or 7.00, respectively, and an internal pH of 6.5 or 6.75 was bactericidal (Fig. 5 E). Together, these results indicate that under normal cecal conditions, SCFAs are sufficient to trigger intracellular acidification in these *K. pneumoniae* and *E. coli* isolates to levels that prevent replication.

Loss of SCFA is associated with expansion of *E. coli* in an allo-HCT patient

The results of our in vivo and in vitro experiments demonstrated that SCFA-mediated intracellular acidification provides coloni-

zation resistance against the tested antibiotic-resistant isolates under our experimental conditions. Therefore, we next asked whether alterations in SCFA levels could also be playing a role in patient populations vulnerable to Enterobacteriaceae expansion. To address this, we examined a patient undergoing allo-HCT who was administered several antibiotics both before and following transplant (Fig. 6 A). Antibiotic administration dramatically altered the fecal microbiota composition and reduced the diversity of bacterial populations, as demonstrated by metagenomic DNA sequence analysis of daily fecal samples (Figs. 6, B and C). Over the course of antibiotic treatment, *E. coli* expanded to abnormally high levels in the intestine (Fig. 6 B). This persistent, abnormally dense intestinal colonization by *E. coli* preceded the development of an *E. coli* BSI (Fig. 6 B), consistent with our previous studies demonstrating that intestinal expansion increases the risk of BSI (Taur et al., 2012). In addition, metagenomic sequencing of fecal samples revealed an increased prevalence of antibiotic resistance genes within in the gut microbiome, coinciding with expansion of *E. coli* before the onset of the BSI (Fig. 6 D). We next measured the concentrations of SCFAs in the daily fecal samples. In line with our observations in mice, as exposure to antibiotics increased over time, SCFA concentrations decreased (Fig. 6 E). Over the first 6 d of treatment, the total SCFA concentration remained above 80 mM (Fig. 6 F), a level of SCFA that strongly inhibited the clinical isolates we tested under in vitro conditions (Fig. 3 B). Furthermore, there was a significant negative correlation between total SCFA concentrations and *E. coli* expansion within the microbiota (Fig. 6 G).

Discussion

Dense colonization of the lower gastrointestinal tract by hospital-associated, antibiotic-resistant strains of Enterobacteriaceae in the colon is an important clinical concern because it increases the risk of disseminated infection, including bacteremia, and it contributes to spread between patients (Taur et al., 2012). Our results suggest that maintenance of an acidic environment coupled with production of high concentrations of SCFA by the cecal and colonic microbiota is critical in preventing the expansion and promoting clearance of the antibiotic-resistant isolates of *K. pneumoniae*, *E. coli*, and *P. mirabilis*. Furthermore, at least with respect to the carbapenem-resistant *K. pneumoniae* strain studied in this report, colonization resistance is not mediated by competition for nutrients and does not require direct antagonism through contact-dependent mechanisms.

Our results indicate that production of SCFA is the most critical function of the microbiota in terms of providing colonization resistance against these hospital-associated Enterobacteriaceae strains. Earlier reports have demonstrated that SCFA have indirect contributions to colonization resistance. In these indirect

experiments; one-way ANOVA followed by Dunnett's multiple comparison test to the control LB condition for each isolate). (C) Growth of Enterobacteriaceae isolates in LB at the indicated pH values with a mixture of acetate, propionate, and butyrate was measured after 16 h of incubation ($n = 6$ wells from two independent experiments). pH values observed directly in cecal contents (Fig. 2 F) are indicated in green (antibiotic naive) or orange (antibiotic treated). Dotted line indicates strain growth in LB alone ($n = 6$ wells from two independent experiments). (D) The *K. pneumoniae*, *E. coli*, or *P. mirabilis* burdens in the intestinal content (CFU/g) of colonized mice given PBS or FMT treatments or collected before treatment is plotted against SCFA concentration in cecal contents (acetate + propionate + butyrate; $n = 3$ –12 mice per group; Spearman correlation. CFU/g values are also plotted in Fig. 1, C and D).

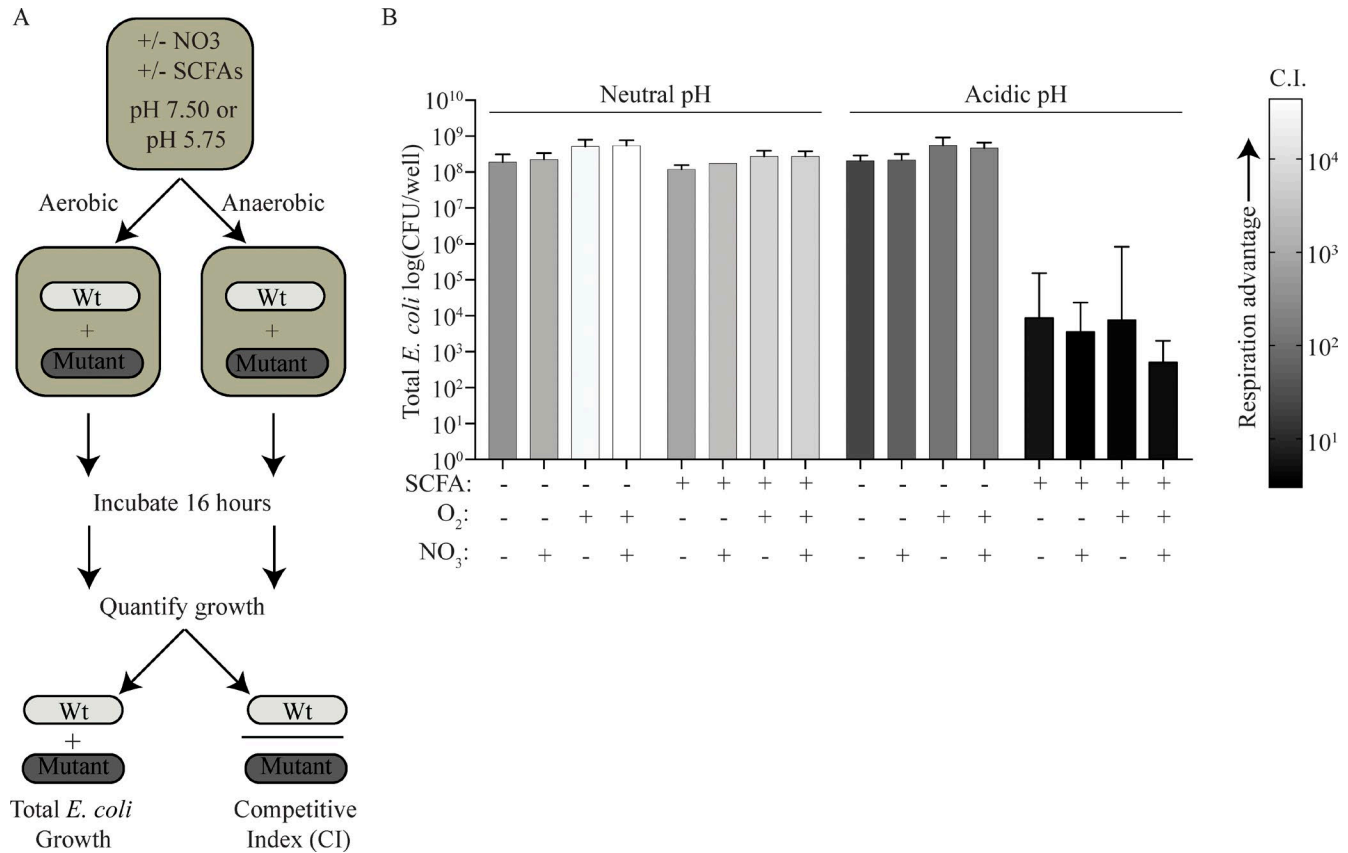


Figure 4. **An acidic pH and SCFA reduce the advantage conferred by aerobic or anaerobic respiration. (A)** Equal numbers of *E. coli* Nissle 1917 and the isogenic *cydAB/napA/narG/narZ* strain were mixed in competitive cultures supplemented with or without SCFAs, NO₃⁻, or oxygen in neutral or acidic pH conditions. Both the total growth of *E. coli* and the competitive advantage of the WT were measured after 16 h. **(B)** The total growth of *E. coli* in the indicated SCFA, NO₃⁻, O₂, and pH conditions is plotted (*n* = 3 wells from three independent experiments, mean + SEM). The shading of each bar indicates the mean competitive advantage of respiration-competent WT compared with the mutant strain for that condition. Values and SEM for the CI are provided in Table S2.

mechanisms, SCFAs function through the activation of host signaling, including peroxisome proliferator-activated receptor-γ, in the host epithelium, leading to reduced oxygen and nitrate availability, which in turn decreases the competitive advantage gained through respiration and also stabilizes HIF-1, leading to production of antimicrobial peptides (Kelly et al., 2013, 2015; Rivera-Chávez et al., 2016; Byndloss et al., 2017). Here, we demonstrate that SCFA can directly trigger the intracellular acidification of *K. pneumoniae* and *E. coli* in the conditions of the lower intestinal tract. While previous in vitro experiments indicated that SCFA can disrupt pH homeostasis in laboratory strains of *E. coli* and *S. Typhimurium* (Wilks and Slonczewski, 2007; Jacobson et al., 2018), our experimental model allowed us to demonstrate for the first time that, directly in the complex mix of solutes present freshly isolated cecal contents, the intracellular pH of carbapenem-resistant *K. pneumoniae* is decreased to a level that prevents replication. Furthermore, this activity is absent in cecal contents from antibiotic-treated mice, but can be rescued by re-introduction of acetate alone.

At physiological concentrations and pH, only acetate and, to a lesser extent, butyrate individually triggered intracellular acidification of carbapenem-resistant *K. pneumoniae* (Fig. 5 and Fig. S4). In contrast, a recent report demonstrated that inhibition of *S. Typhimurium* replication depends on propionate-driven in-

tracellular acidification (Jacobson et al., 2018). We also observed moderate strain-specific variation in the degree of SCFA-mediated inhibition in acidic pH conditions (Fig. 3C). Together, these data suggest that overall susceptibility to the Enterobacteriaceae family is likely determined by total concentrations of SCFAs, but that variations in the amounts of individual SCFA might differentially influence susceptibility to different species of Enterobacteriaceae. In addition, pH has been reported to play a role in shaping the balance between Bacteroidetes and Firmicutes in in vitro assays (Duncan et al., 2009), raising the possibility that changes in acetate, propionate, and butyrate ratios or levels along with pH might also influence the composition of the indigenous microbiota. In future studies, it will be informative to determine if differences in membrane permeability, or the presence of specific pathways allowing for tolerance or reversal of intracellular pH stresses represent mechanisms of differential sensitivity.

One of the differences between Enterobacteriaceae and the Firmicutes and Bacteroidetes is the ability of Enterobacteriaceae to use oxygen, nitrates, and other substrates as terminal electron acceptors enabling aerobic and anaerobic respiration. In contrast, many Firmicutes and Bacteroidetes derive energy through fermentation pathways. We demonstrate that the products of microbiota fermentation, SCFAs, markedly reduce the

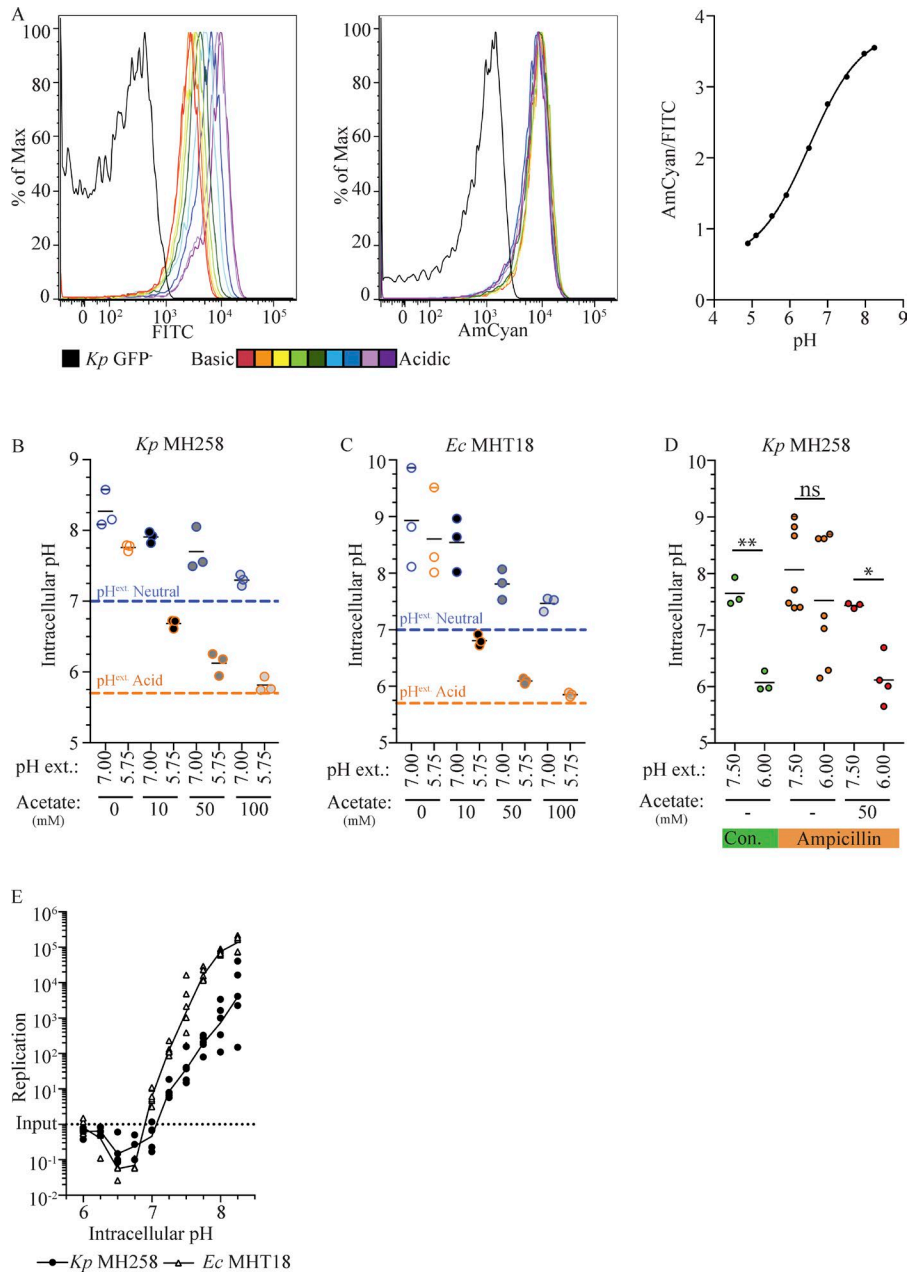
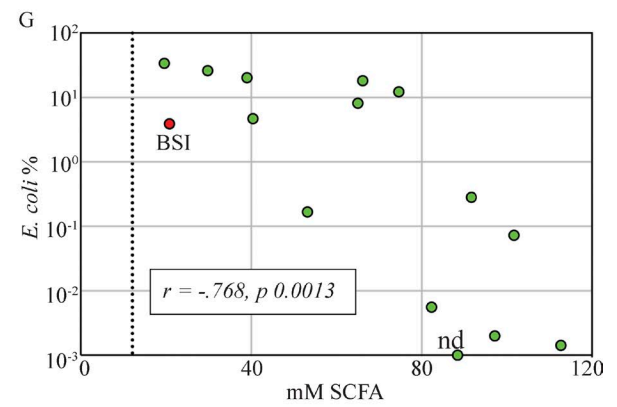
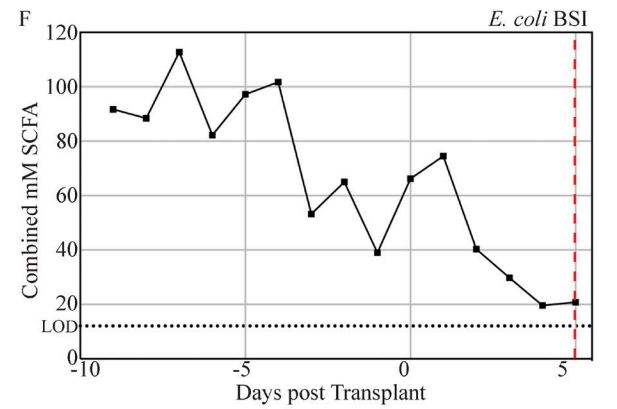
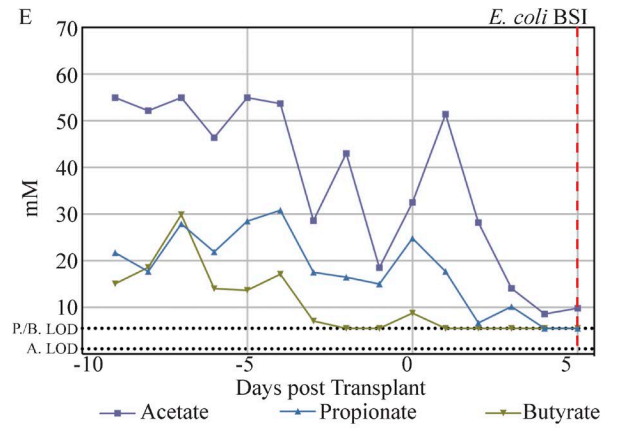
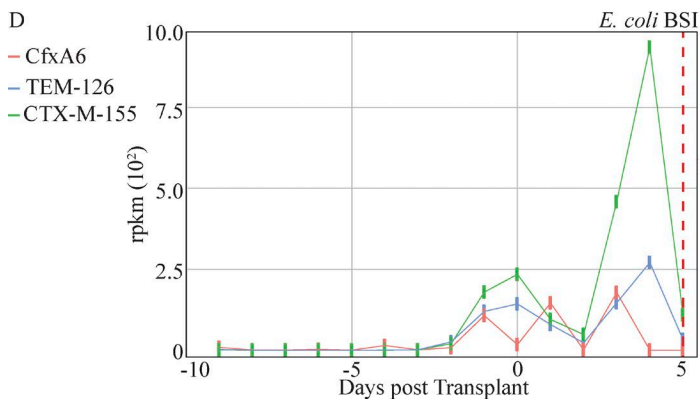
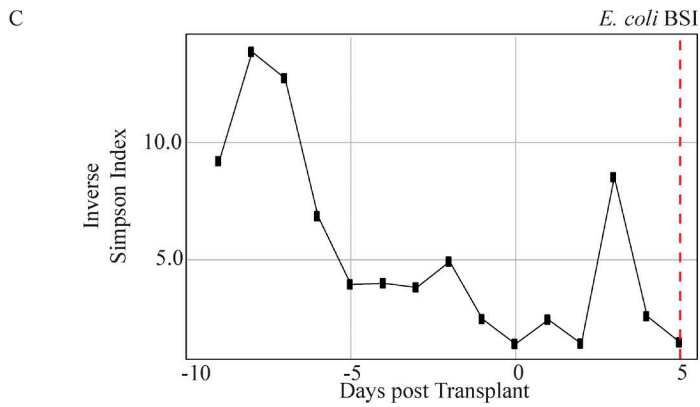
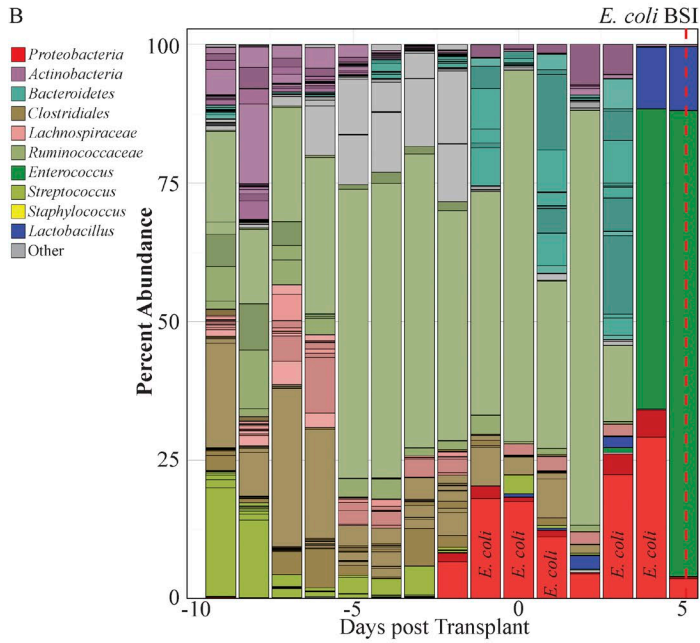
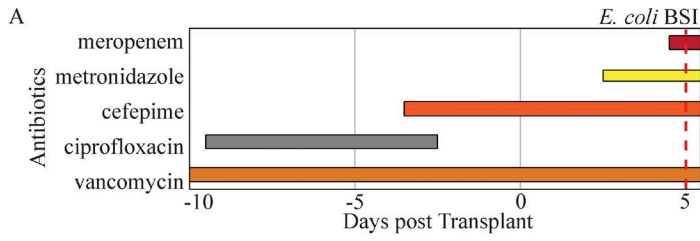


Figure 5. SCFA prevent *E. coli* and *K. pneumoniae* replication by decreasing intracellular pH. (A) Representative histograms of FITC and AmCyan fluorescence of pHlourin-expressing *K. pneumoniae* MH258 at different set pH values in the presence of potassium benzoate and methylamine hydrochloride (left). A representative standard curve depicting the relationship between intracellular pH and AmCyan/FITC intensity ratios (right). (B and C) The intracellular pH of *K. pneumoniae* MH258 (B) or *E. coli* MHT18 (C) in the presence of the indicated concentrations of acetate in LB at pH 7.0 or 5.75 ($n = 3$ from three independent experiments). (D) The intracellular pH of *K. pneumoniae* MH258 in freshly isolated cecal contents from control or antibiotic-treated mice supplemented with 50 mM of acetate as indicated. External pH was set at 7.5 or 6.0 as indicated ($n = 3-7$ from three to seven independent experiments; t test). In B-D, values above the upper limit of confidence are indicated with a horizontal line. (E) Anaerobic replication of *K. pneumoniae* MH258 or *E. coli* MHT18 in LB with potassium benzoate and methylamine hydrochloride at the indicated pH levels ($n = 3-6$ wells from three to four independent experiments). *Ec*, *E. coli*; *Kp*, *K. pneumoniae*; *Pm*, *P. mirabilis*.

competitive advantage Enterobacteriaceae gain through respiration compared with respiration-deficient strains. Our observations suggest a model in which, during antibiotic-mediated destruction of the microbiota, the luminal environment transitions from a state characterized by an acidified pH with high SCFA and low oxygen and nitrates to a neutral environment with higher oxygen and nitrate availability and low SCFAs. Our mechanistic studies indicate that during this transition, it is the loss of SCFA production and the acidic pH that enables Enterobacteriaceae replication. As previously reported, during this transition, the competitive advantage gained through respiration increases as a result of oxygen and nitrate availability. Our study extends this finding, by demonstrating that the transition from an acidic to neutral pH is also critical in creating an environment that confers the maximum advantage for respiration-competent strains.

In addition to providing colonization resistance, our data demonstrates that clearance of established populations of *K. pneumoniae*, *E. coli*, and *P. mirabilis* in the noninflamed colon is associated with a recovery of SCFA production by the microbiota. In our mouse model, the microbiota partially recovers and begins producing SCFA without intervention following the cessation of antibiotic treatment (Fig. 3 D and Fig. S3). However, therapeutic intervention by administration of a complex microbiota drives more complete microbiota recovery (Fig. S1 B) and rescues SCFA production (Fig. 3 D and Fig. S3), leading to a significant reduction in colonization by *K. pneumoniae*, *E. coli*, and *P. mirabilis* (Fig. 1, C-E). Our findings show that a similar loss of SCFA and disruption of the microbiota can occur with antibiotic treatment in patients (Fig. 6). Earlier studies in pediatric patients undergoing allo-HCT demonstrated, in the absence of therapeutic intervention, that alterations in the composition of the microbiota



can persist for months following treatment (Biagi et al., 2015). This suggests that patients might benefit from therapeutic intervention with complex microbiotas or defined communities specifically selected to rapidly rescue total SCFA production as well as colonic acidification to reduce the risk of Enterobacteriaceae BSIs. In line with this, two recent clinical studies have demonstrated that third-party or autologous FMT treatments can safely increase microbiota diversity in allo-HCT patients (DeFilipp et al., 2018; Taur et al., 2018). Our work indicates that the capacity to acidify the proximal colon and produce high concentrations of SCFA is likely to be a critical parameter in the success of therapeutic microbiota interventions in preventing the abnormal expansion of antibiotic-resistant *K. pneumoniae* or *E. coli*.

Materials and methods

Patient sample collection

Fecal samples were collected from an adult patient undergoing allo-HCT at Memorial Sloan Kettering Cancer Center. The patient was enrolled in a prospective fecal collection protocol, where fecal samples are collected from patients during transplant hospitalization in a biospecimen bank, as previously described (Taur et al., 2012). The study was approved by the Institutional Review Board at Memorial Sloan Kettering Cancer Center. All study patients provided written informed consent for biospecimen collection and analysis. The study was conducted in accordance with the Declaration of Helsinki. The fecal samples studied here were selected for metagenomics and metabolomics processing retrospectively on the basis of the patient's development of a BSI with *E. coli*.

Bacterial strains

The *E. coli* MHT18 and MHX43 isolates and *P. mirabilis* MH438 and MH42F isolates were isolated by the Clinical Microbiology Service at Memorial Hospital, Memorial Sloan Kettering Cancer Center. Antimicrobial susceptibility testing of these isolates was performed using a Neg MIC 43 panel on a Microscan System (Beckman Coulter) by the Clinical Microbiology Service at Memorial Hospital. The *K. pneumoniae* MH258 and MH189 isolates were previously described (Xiong et al., 2015). These isolates of *K. pneumoniae*, *E. coli*, and *P. mirabilis* were routinely grown overnight in LB broth (BD) with 100 µg/ml ampicillin (Fisher Scientific) at 37°C under aerobic conditions. *E. coli* Nissle 1917 and the isogenic *E. coli* Nissle 1917 *cydAB/napA/narG/narZ* strain were routinely grown in LB broth as previously described (Byndloss et al., 2017).

Mice

6–8-wk-old C57BL/6 (WT) female mice were purchased from The Jackson Laboratory and then maintained under specific patho-

gen-free conditions at the Memorial Sloan Kettering Research Animal Resource Center. Male and female gnotobiotic mice were bred in house and maintained in gnotobiotic isolators before being transferred to cages under specific pathogen-free conditions for treatment. All animal procedures were approved by the Institutional Animal Care and Use Committee of the Memorial Sloan Kettering Cancer Center.

Colonization resistance against Enterobacteriaceae

WT mice were given ampicillin in sterile drinking water at a concentration of 500 mg/liter for 4 d (day –4 to day 0). Control mice were kept on sterile drinking water. On the day of challenge (day 0), overnight cultures of *K. pneumoniae* MH258, *E. coli* MHT18, and *P. mirabilis* MH42F were diluted 1:20 and grown with shaking at 37°C for 2 h before dilution. Mice were individually housed in autoclaved cages without ampicillin in the drinking water and were challenged with ~500–1,000 CFUs in 200 µl of PBS by oral gavage. Fecal pellets were collected from ampicillin-treated and antibiotic-naive mice at 1 and 3 d after challenge. Pellets were resuspended at 50 mg/ml in PBS, diluted, and plated on LB agar plates with 100 µg/ml ampicillin.

Individually housed gnotobiotic mice were gavaged with 200 µl of an FMT from a WT mouse or PBS as a control (day –12). FMTs were prepared by collecting cecal contents from WT mice under anaerobic conditions in an anaerobic chamber (Coylabs). Cecal contents were then resuspended at 200 mg/ml in reduced PBS with 10% glycerol before freezing at –80°C. After 12 d, mice were challenged with 500–1,000 CFUs of *K. pneumoniae* MH258 as described above (day 0). At days 1 to 4 after challenge, pellets were collected and plated as described above to measure *K. pneumoniae* colonization. At days –5 and 0–4, a second set of pellets was collected and immediately frozen for 16S rRNA analysis as described below.

Enterobacteriaceae clearance experiments

WT mice were treated with ampicillin (day –4 to day 0) and challenged with *K. pneumoniae* MH258, *E. coli* MHT18, or *P. mirabilis* MH42F (on day 0) as described above. On days 3, 4, and 5 after challenge, mice were gavaged with 200 µl of PBS or 200 µl of a FMT prepared as described above.

Levels of *K. pneumoniae*, *E. coli*, and *P. mirabilis* colonization were measured by collecting and plating fecal pellets as described above. Colonization was measured at days –4 and 0 to confirm that no colonization was detectable before Enterobacteriaceae challenge. Samples were then taken at day 3 and then every 2 d thereafter to monitor clearance.

At days –4, 0, 3, 7, and 17, a second set of fecal pellet samples was collected and immediately frozen on dry ice for Illumina

Figure 6. **Loss of SCFA production correlates with *E. coli* expansion in an allo-HCT patient.** (A) Daily changes in the composition of the intestinal microbiota were monitored in a patient undergoing allo-HCT from 9 d before transplant to 5 d after transplant when a BSI with *E. coli* was detected (dashed red line). Select antibiotics administered to the patient are depicted. (B) The composition of the microbiota in daily fecal samples is plotted. Values are plotted as the percent abundance of each species determined using MetaPhlAn analysis. (C) The inverse Simpson diversity index of the microbiota in daily fecal samples. (D) Levels of the indicated β-lactamase genes in the microbiota from daily fecal samples. (E) Acetate, propionate, and butyrate concentrations in daily fecal samples from the patient. (F) Total SCFA in daily fecal samples from the patient calculated as the sum of acetate, propionate, and butyrate. (G) The relative abundance of *E. coli* (MetaPhlAn) compared with the total SCFA concentration in the daily fecal sample. At the point highlighted in red, a BSI with *E. coli* was detected ($n = 15$ d; Spearman correlation).

MiSeq analysis as described below. On day 17, mice were sacrificed, and a sample of cecal contents was frozen at -80°C for SCFA analysis as described below. Successful FMT treatment was defined as an Enterobacteriaceae load of less than 10^7 CFU/g at day 17. To assess SCFA concentrations at the peak of colonization, a third group of mice was sacrificed at day 3 after colonization (before FMT treatment), and a sample of cecal contents was collected as above.

16S rRNA sequencing

DNA was isolated from murine fecal pellets or patient fecal samples using 0.1-mm zirconia/silica beads (BioSpec Products) to homogenize the sample and phenol/chloroform/isoamyl extraction as previously described (Becattini et al., 2017). After phenol/chloroform/isoamyl extraction, DNA was precipitated in ethanol, resuspended in TE buffer with 200 $\mu\text{g}/\text{ml}$ RNase, and further purified with QIAamp mini spin columns (Qiagen). The V4–V5 region of the 16S rRNA gene was amplified with the primers 563F (5'-nnnnnnnn-NNNNNNNNNNNN-AYTGGGYDTAAAGNG-3') and 926R (5'-nnnnnnnn-NNNNNNNNNNNN-CCGTC AATTYHTTTRAGT-3'), where uppercase Ns represent 12-bp Golay barcodes and lowercase Ns represent additional nucleotides to offset the sequencing of the primers (Caporaso et al., 2012). Amplicons were purified with the Qiaquick PCR Purification kit (Qiagen). The purified PCR products were quantified using Agilent Technologies 2200 tape station and pooled at equimolar amounts. The TruSeq DNA library preparation kit (Illumina) was used according to the manufacturer's instructions to prepare the library. The library was sequenced on an Illumina MiSeq platform following the manufacturer's instructions and a paired-end 250 \times 250-bp kit.

16S rRNA phylogenetic analysis

16S rRNA (V4–V5) paired end reads were merged and de-multiplexed. Maximum expected error filtering ($E_{\text{max}} = 1$; Edgar and Flyvbjerg, 2015), operational taxonomic unit (OTU) grouping (97% distance-based similarity), and chimeric and singleton sequence removal were performed using the UPARSE pipeline (Edgar, 2013). Taxonomic classification of OTUs was performed by nucleotide BLAST of representative sequences from each OTU, with NCBI RefSeq as the reference training set. A minimum E-value threshold value of $1e-10$ was used for assignments. Species abundances were plotted as the proportion of 16S rRNA sequences (Fig. S1 A), or unweighted UniFrac analyses or Simpson diversity analyses were performed using the phyloseq R package (Fig. S1 B and Fig. 6 C; McMurdie and Holmes, 2013).

Metagenomic sequencing

DNA was isolated from fecal samples as described above. After purification using the QIAamp mini spin columns, the purified DNA was quantified. 1 μg of DNA in a volume of 50 μl of H_2O was sheared to a target size of 650 bp with an Ultrasonicator (Covaris). Following shearing, size selection with AMPure XP beads (Beckman Coulter) was performed and libraries were prepared for sequencing with the TruSeq DNA library preparation kit according to the manufacturer's instructions (Illumina). Sequencing was performed on a HiSeq platform (Illumina) with a

paired-end 100 \times 100-bp kit in pools designed to provide 20–30 million reads per sample.

Metagenome analysis

Whole metagenome data were trimmed and human reads were filtered with KneadData (version 0.5.1) using default settings and removing reads <70 bp. Community composition was calculated using MetaPhlan2 (version 20; Truong et al., 2015) using the default settings. Antibiotic resistance genes were identified using Short, Better Representative Extract Dataset (ShortBRED; Kaminski et al., 2015). First, ShortBRED-identify was used to create a database of unique marker peptide sequences of antibiotic resistance genes from the Comprehensive Antibiotic Resistance Database version 1.2.1 (Jia et al., 2017). The UniRef90 protein database was used to define unique peptide marker sequences. Lastly, ShortBRED-quantify was used to map translated reads to protein markers using the default parameters.

SCFA analysis

Concentrations of acetate, propionate, and butyrate were measured as previously described (Haak et al., 2018). In brief, murine cecal content samples were collected directly into Bead-Ruptor tubes with 2.8-mm ceramic beads (OMNI International) and immediately frozen on dry ice. For patient samples, frozen fecal samples were aliquoted into Bead-Ruptor tubes. After thawing, samples were extracted with 80% methanol containing internal standards of deuterated SCFA (D-3 acetate, D-5 propionate, and D-7 butyrate; Cambridge Isotope Laboratories). Pellets were resuspended at a ratio of 100 mg/ml and homogenized. Homogenized samples were centrifuged at 20,000 g for 15 min at 4°C . The supernatant was derivatized for 60 min at 65°C with one volume of 50 mM, pH 11.0 borate buffer, and four volumes of 100 mM pentafluorobenzyl bromide (Thermo Scientific) in acetone (Fisher Scientific). The SCFA were extracted in n-hexane and then further diluted 1:10 in n-hexane. Extracted SCFA were quantified by GCMS (Agilent 7890A GC System; Agilent 5975C MS detector) operating in negative chemical ionization mode with methane as the reagent gas. MassHunter software was used for data analysis (B07.0; Agilent Technologies).

Ex vivo cecal content cultures

WT mice were kept on sterile water or sterile water with ampicillin (500 mg/liter). After 3 d, mice were sacrificed and cecal contents were collected anaerobically and resuspended at 250 mg/ml in PBS. These cultures were incubated at 37°C for 24 h under anaerobic conditions. After 24 h, cultures were either inoculated with *K. pneumoniae*, *E. coli*, or *P. mirabilis* directly (as described below) or a portion of the cultures was used to prepare supernatants. Culture supernatants were prepared by centrifuging the contents at 10,000 g for 2 min and then filtering the supernatant through a 0.22- μm filter. For conditions with neutralized control contents, the pH of the control supernatant was titrated to 7.0 with NaOH. For conditions with acidified ampicillin contents, the pH of the ampicillin supernatant was titrated to 5.75 with HCl. For dilution experiments, culture supernatants from antibiotic-naive mice were diluted in PBS.

Stationary phase cultures of *K. pneumoniae*, *E. coli*, or *P. mirabilis* were serially diluted to 10^{-5} and then 1:2. 40 μ l of this dilution was added to 180 μ l of PBS, antibiotic-naive or ampicillin-treated cecal content cultures. For supernatant conditions, stationary phase cultures of *K. pneumoniae*, *E. coli*, and *P. mirabilis* were serially diluted to 10^{-3} in PBS and then 10^{-4} and 10^{-5} in each supernatant condition. 20 μ l of the 10^{-5} dilution was added to 200 μ l of the appropriate supernatant. All cultures were then incubated overnight at 37°C. After 24 h, samples were serially diluted and plated on LB agar + 100 μ g/ml ampicillin to measure *K. pneumoniae*, *E. coli*, or *P. mirabilis* growth.

SCFA in vitro inhibition

To model in vivo SCFA concentrations, 50 mM acetic acid, 6 mM propionic acid, and 25 mM butyric acid were added to LB. LB or LB + SCFA was then titrated to pH 5.75, 6.00, 6.25, 6.50, 6.75, or 7.0 with NaOH and HCl, filtered through a 0.22- μ m filter and allowed to reduce in an anaerobic chamber. Overnight cultures of *K. pneumoniae*, *E. coli*, or *P. mirabilis* strains, grown under anaerobic conditions, were diluted to 10^{-3} in LB and further diluted to 10^{-5} in reduced LB or LB + SCFA. 200 μ l of LB or LB + SCFA at pH 5.75 or 7.00 were inoculated with the diluted *K. pneumoniae*, *E. coli*, and *P. mirabilis* and incubated for 16 h at 37°C under anaerobic conditions. Growth was measured by serial dilution and plating on LB agar + ampicillin plates.

CI assays

LB and LB + SCFA were prepared as described above. For conditions with nitrates, NaNO₃ was added at a final concentration of 1 mM. The pH of the solutions was adjusted to pH 5.75 or 7.50 with HCl and NaOH. After filtering through a 0.22- μ m filter, solutions were transferred into an anaerobic chamber or left aerobic. Cecal content culture supernatants from antibiotic-naive or ampicillin-treated mice were prepared as described above. Where indicated, 50 mM of acetate, 6 mM of propionate, and 25 mM of butyrate were added. pH was adjusted to 5.75 or 7.50 or left at the naturally occurring pH as indicated. After filtering through a 0.22- μ m filter, solutions were transferred into an anaerobic chamber or left aerobic. The OD_{600nm} densities of overnight cultures of WT *E. coli* Nissle or the *cydAB/napA/narG/narX* strain (mutant) were measured, and an equal amount of each strain was mixed. Under aerobic or anaerobic conditions, as indicated, the mixture was then serially diluted to 10^{-3} in LB and further diluted to 10^{-5} in each assay condition. The diluted mixture of WT and mutant *E. coli* was plated on LB agar with carbenicillin and streptomycin with or without kanamycin to measure the input CFU of the WT and mutant *E. coli*, respectively. 20 μ l of the dilution was used to inoculate 200 μ l of each assay condition, and growth of the WT and mutant strains was measured by plating on selective media after 16 h. CI values were calculated as: $(WT_{16h} / mutant_{16h}) / (WT_{input} / mutant_{input})$.

Construction of pHluorin-arr-3 plasmid

The arr-3 gene encoding rifampicin resistance was amplified by PCR from a pKD46-arr-3 plasmid template using primers with the sequence 5'-TGAAAAAGGAAGAGTATGGTAAAAGATTGGATTCCCATC-3' and 5'-AACTTGGTCTGACAGCTAGTCTCAATGAC

GTGTAAACC-3'. The pHluorin-expressing plasmid pGFPRO1 (Martinez et al., 2012) was linearized by PCR with the primers 5'-ACTCTTCCTTTTCAATATTATTG-3' and 5'-CTGTGACACCAAGTTTACTCAT-3'. PCR products were purified by gel extraction (Qiagen). The amplified arr-3 gene was ligated into the linearized vector using the IN-Fusion HD cloning kit according to the manufacturer's instructions (Clontech; Takara Bio USA). The ligated plasmid was transformed into Stellar-competent cells (Clontech; Takara Bio USA). Transformed cells were selected for on LB agar with rifampin at 50 μ g/ml (Rifadin IV; Novaplus). Miniprep purified pHluorin-arr-3 plasmid was transformed by electroporation into the *K. pneumoniae* MH258 and *E. coli* MHT18 isolates.

Intracellular pH measurement

K. pneumoniae MH258-pGFP or *E. coli* MHT18 were grown to stationary phase in the presence of rifampicin at 37°C. Stationary phase cultures were diluted 1:20 into LB media with rifampicin and 1% L-arabinose and incubated at 37°C with shaking. After 2 h, log phase cultures were used in intracellular pH assays.

Assay conditions were prepared fresh for each experiment. For in vitro assays, sodium acetate, propionic acid, or butyric acid were added to cultures at 100, 50, or 10 mM. LB with or without these SCFA was titrated to a pH of 7.00 or 5.75. For ex vivo assays, cecal contents from antibiotic-naive or ampicillin-treated mice were collected and resuspended at a ratio of 750 mg/ml in ddH₂O. The resuspended contents were centrifuged at 10,000 g for 2 min and filtered through a 0.22- μ m filter. The pH was then adjusted to pH 6.0 or 7.5. To generate standard curves, 40 mM potassium benzoate and 40 mM methylamine hydrochloride were added, and the pH was adjusted to set pH values.

Log phase cultures were serially diluted in each assay condition to 10^{-3} and allowed to sit for 4 min at room temperature. GFP fluorescence was then analyzed by flow cytometry on a LSRII flow cytometer (BD). Data were collected using BD FACS DIVA v8.0.1 and analyzed with FlowJo v9.9. Bacteria were selected by forward scatter and side scatter gating, and pH-sensitive GFP fluorescence was measured in the AmCyan and FITC channels. At least 10^3 bacterial cells were analyzed.

The ratios of background-subtracted mean fluorescence intensities of the GFP and AmCyan channels in conditions with potassium benzoate and methylamine-hydrochloride at set pH values were used to generate a standard curve. A Boltzmann-sigmoidal curve was used to fit the data (Martinez et al., 2012). Independent standard curves were generated in each experiment and for each starting solution (LB, antibiotic-naive supernatant, ampicillin-treated supernatant).

Statistical methods

Individual data points are depicted throughout the paper; in some cases the geometric mean is also indicated with a solid line. In Fig. 4, Fig. S4, and Table S2, the mean and SEM were calculated on the log-transformed values of both *E. coli* CFU/well and the CI. Analyses were performed with GraphPad Prism version 7.0a or R-3.3.2.pkg. Statistical tests included *t* tests with Holm-Sidak correction for multiple comparisons, one-way ANOVA followed by either Dunnett's multiple comparison test to a control sample or Sidak's multiple comparison test between selected pairs of

conditions, unpaired *t* test, and spearman correlation analysis, as indicated in figure legends. Statistical tests on values of CFU/g or CFU/well were performed on log-transformed data. A Boltzmann-sigmoidal curve was used to fit the intracellular pH curve.

Data availability

Sequence data that support the findings of this study are available as an NCBI BioProject (ID: PRJNA479462).

Online supplemental material

Fig. S1 shows the microbiota composition in reconstituted gnotobiotic mice and Enterobacteriaceae-colonized mice receiving FMT treatments. Fig. S2 shows the inhibition of Enterobacteriaceae expansion in cecal content cultures. Fig. S3 shows the SCFA levels in Enterobacteriaceae-colonized mice following PBS or FMT treatment. Fig. S4 shows the growth of WT and respiration-deficient *E. coli* in cecal content cultures under different oxygen, SCFA, and pH conditions. Fig. S5 shows in the intracellular pH of *K. pneumoniae* MH258 in the presence of increasing concentrations of propionate and butyrate. Table S1 shows the antimicrobial resistance profile of selected Enterobacteriaceae strains. Table S2 shows the CI values of WT over respiration-deficient *E. coli* in broth and cecal content cultures.

Acknowledgments

The pKD46-arr-3 plasmid was a gift from Dr. L. Chen (Rutgers New Jersey Medical School, Newark, NJ). The pGFPPO1 plasmid was a gift from Dr. J.L. Slonczewski (Kenyon College, Gambier, OH).

M.T. Sorbara is supported by a Canadian Institute of Health Research Fellowship (FRN#152527). E.G. Pamer has received funding from National Institutes of Health grants R01 AI042135, AI095706, U01 AI124275, and P30 CA008748.

J.U. Peled receives research support and licensing fees from Seres Therapeutics. M.R.M. van den Brink has received speaker honoraria from Flagship Ventures, Novartis, Evelo, Jazz Pharmaceuticals, Therakos, Amgen, Merck & Co. Inc., and Acute Leukemia Forum; is an advisor for and receives research support and licensing fees from Seres Therapeutics; receives licensing fees from Juno Therapeutics; and serves on the DKMS Medical Council Board. E.G. Pamer has received speaker honoraria from Bristol Myers Squibb, Celgene, Seres Therapeutics, MedImmune, Novartis, and Ferring Pharmaceuticals and is an inventor on patent application no. WPO2015179437A1, entitled “Methods and compositions for reducing *Clostridium difficile* infection,” and no. WO2017091753A1, entitled “Methods and compositions for reducing vancomycin-resistant enterococci infection or colonization,” and holds patents that receive royalties from Seres Therapeutics. The authors declare no further competing financial interests.

Author contributions: M.T. Sorbara and E.G. Pamer conceptualized the study and designed experiments. M.T. Sorbara, K. Dubin, T.U. Moody, E. Fontana, R. Seok, and I.M. Leiner performed experiments. M.T. Sorbara analyzed and interpreted data throughout the paper; E.R. Littmann and T.U. Moody analyzed 16S sequencing results, and A.J. Pickard, J.-L. Chaubard, and J.R. Cross analyzed SCFA measurements. J.U. Peled, M.R. van den Brink, and Y. Taur

established the patient sample collection protocol and maintained the biospecimen bank. Y. Litvak and A.J. Bäumler provided critical resources. M.T. Sorbara and E.G. Pamer wrote the manuscript.

Submitted: 24 August 2018

Revised: 26 October 2018

Accepted: 7 December 2018

References

- Becattini, S., E.R. Littmann, R.A. Carter, S.G. Kim, S.M. Morjaria, L. Ling, Y. Gyaltsen, E. Fontana, Y. Taur, I.M. Leiner, and E.G. Pamer. 2017. Commensal microbes provide first line defense against *Listeria monocytogenes* infection. *J. Exp. Med.* 214:1973–1989. <https://doi.org/10.1084/jem.20170495>
- Biagi, E., D. Zama, C. Nastasi, C. Consolandi, J. Fiori, S. Rampelli, S. Turroni, M. Centanni, M. Severgnini, C. Peano, et al. 2015. Gut microbiota trajectory in pediatric patients undergoing hematopoietic SCT. *Bone Marrow Transplant.* 50:992–998. <https://doi.org/10.1038/bmt.2015.16>
- Bohnhoff, M., C.P. Miller, and W.R. Martin. 1964a. Resistance of the Mouse's Intestinal Tract to Experimental Salmonella Infection. I. Factors Which Interfere with the Initiation of Infection by Oral Inoculation. *J. Exp. Med.* 120:805–816. <https://doi.org/10.1084/jem.120.5.805>
- Bohnhoff, M., C.P. Miller, and W.R. Martin. 1964b. Resistance of the Mouse's Intestinal Tract to Experimental Salmonella Infection. II. Factors Responsible for Its Loss Following Streptomycin Treatment. *J. Exp. Med.* 120:817–828. <https://doi.org/10.1084/jem.120.5.817>
- Buffie, C.G., and E.G. Pamer. 2013. Microbiota-mediated colonization resistance against intestinal pathogens. *Nat. Rev. Immunol.* 13:790–801. <https://doi.org/10.1038/nri3535>
- Byndloss, M.X., E.E. Olsan, F. Rivera-Chávez, C.R. Tiffany, S.A. Cevallos, K.L. Lokken, T.P. Torres, A.J. Byndloss, F. Faber, Y. Gao, et al. 2017. Microbiota-activated PPAR- γ signaling inhibits dysbiotic Enterobacteriaceae expansion. *Science.* 357:570–575. <https://doi.org/10.1126/science.aam9949>
- Caporaso, J.G., C.L. Lauber, W.A. Walters, D. Berg-Lyons, J. Huntley, N. Fierer, S.M. Owens, J. Betley, L. Fraser, M. Bauer, et al. 2012. Ultra-high-throughput microbial community analysis on the Illumina HiSeq and MiSeq platforms. *ISME J.* 6:1621–1624. <https://doi.org/10.1038/ismej.2012.8>
- Centers for Disease Control and Prevention. 2013. Antibiotic Resistance Threats in the United States. <https://www.cdc.gov/drugresistance/threat-report-2013/pdf/ar-threats-2013-508.pdf> (accessed August 1, 2018)
- DeFilipp, Z., J.U. Peled, S. Li, J. Mahabamunuge, Z. Dagher, A.E. Slingerland, C. Del Rio, B. Valles, M.E. Kempner, M. Smith, et al. 2018. Third-party fecal microbiota transplantation following allo-HCT reconstitutes microbiome diversity. *Blood Adv.* 2:745–753. <https://doi.org/10.1182/bloodadvances.2018017731>
- den Besten, G., K. van Eunen, A.K. Groen, K. Venema, D.J. Reijngoud, and B.M. Bakker. 2013. The role of short-chain fatty acids in the interplay between diet, gut microbiota, and host energy metabolism. *J. Lipid Res.* 54:2325–2340. <https://doi.org/10.1194/jlr.R036012>
- Duncan, S.H., P. Louis, J.M. Thomson, and H.J. Flint. 2009. The role of pH in determining the species composition of the human colonic microbiota. *Environ. Microbiol.* 11:2112–2122. <https://doi.org/10.1111/j.1462-2920.2009.01931.x>
- Edgar, R.C. 2013. UPARSE: highly accurate OTU sequences from microbial amplicon reads. *Nat. Methods.* 10:996–998. <https://doi.org/10.1038/nmeth.2604>
- Edgar, R.C., and H. Flyvbjerg. 2015. Error filtering, pair assembly and error correction for next-generation sequencing reads. *Bioinformatics.* 31:3476–3482. <https://doi.org/10.1093/bioinformatics/btv401>
- Farmer, A.D., S.D. Mohammed, G.E. Dukes, S.M. Scott, and A.R. Hobson. 2014. Caecal pH is a biomarker of excessive colonic fermentation. *World J. Gastroenterol.* 20:5000–5007. <https://doi.org/10.3748/wjg.v20.i17.5000>
- Gantois, I., R. Ducatelle, F. Pasmans, F. Haesebrouck, I. Hautefort, A. Thompson, J.C. Hinton, and F. Van Immerseel. 2006. Butyrate specifically down-regulates salmonella pathogenicity island 1 gene expression. *Appl. Environ. Microbiol.* 72:946–949. <https://doi.org/10.1128/AEM.72.1.946-949.2006>
- Haak, B.W., E.R. Littmann, J.L. Chaubard, A.J. Pickard, E. Fontana, F. Adhi, Y. Gyaltsen, L. Ling, S.M. Morjaria, J.U. Peled, et al. 2018. Impact of gut

- colonization with butyrate-producing microbiota on respiratory viral infection following allo-HCT. *Blood*. 131:2978–2986.
- Hecht, A.L., B.W. Casterline, Z.M. Earley, Y.A. Goo, D.R. Goodlett, and J. Bubeck Wardenburg. 2016. Strain competition restricts colonization of an enteric pathogen and prevents colitis. *EMBO Rep*. 17:1281–1291. <https://doi.org/10.15252/embr.201642282>
- Human Microbiome Project Consortium. 2012. Structure, function and diversity of the healthy human microbiome. *Nature*. 486:207–214. <https://doi.org/10.1038/nature11234>
- Jacobson, A., L. Lam, M. Rajendram, F. Tamburini, J. Honeycutt, T. Pham, W. Van Treuren, K. Pruss, S.R. Stabler, K. Lugo, et al. 2018. A Gut Commensal-Produced Metabolite Mediates Colonization Resistance to Salmonella Infection. *Cell Host Microbe*. 24:296–307.e7. <https://doi.org/10.1016/j.chom.2018.07.002>
- Jia, B., A.R. Raphenya, B. Alcock, N. Waglechner, P. Guo, K.K. Tsang, B.A. Lago, B.M. Dave, S. Pereira, A.N. Sharma, et al. 2017. CARD 2017: expansion and model-centric curation of the comprehensive antibiotic resistance database. *Nucleic Acids Res*. 45(D1):D566–D573. <https://doi.org/10.1093/nar/gkw1004>
- Kamada, N., Y.G. Kim, H.P. Sham, B.A. Vallance, J.L. Puente, E.C. Martens, and G. Núñez. 2012. Regulated virulence controls the ability of a pathogen to compete with the gut microbiota. *Science*. 336:1325–1329. <https://doi.org/10.1126/science.1222195>
- Kaminski, J., M.K. Gibson, E.A. Franzosa, N. Segata, G. Dantas, and C. Huttenhower. 2015. High-Specificity Targeted Functional Profiling in Microbial Communities with ShortBRED. *PLoS Comput. Biol*. 11:e1004557. <https://doi.org/10.1371/journal.pcbi.1004557>
- Kelly, C.J., L.E. Glover, E.L. Campbell, D.J. Kominsky, S.F. Ehrentraut, B.E. Bowers, A.J. Bayless, B.J. Saeedi, and S.P. Colgan. 2013. Fundamental role for HIF-1 α in constitutive expression of human β defensin-1. *Mucosal Immunol*. 6:1110–1118. <https://doi.org/10.1038/mi.2013.6>
- Kelly, C.J., L. Zheng, E.L. Campbell, B. Saeedi, C.C. Scholz, A.J. Bayless, K.E. Wilson, L.E. Glover, D.J. Kominsky, A. Magnuson, et al. 2015. Crosstalk between Microbiota-Derived Short-Chain Fatty Acids and Intestinal Epithelial HIF Augments Tissue Barrier Function. *Cell Host Microbe*. 17:662–671. <https://doi.org/10.1016/j.chom.2015.03.005>
- Kim, S., A. Covington, and E.G. Pamer. 2017. The intestinal microbiota: Antibiotics, colonization resistance, and enteric pathogens. *Immunol. Rev*. 279:90–105. <https://doi.org/10.1111/imr.12563>
- Lawhon, S.D., R. Maurer, M. Suyemoto, and C. Altier. 2002. Intestinal short-chain fatty acids alter Salmonella typhimurium invasion gene expression and virulence through BarA/SirA. *Mol. Microbiol*. 46:1451–1464. <https://doi.org/10.1046/j.1365-2958.2002.03268.x>
- Luli, G.W., and W.R. Strohl. 1990. Comparison of growth, acetate production, and acetate inhibition of Escherichia coli strains in batch and fed-batch fermentations. *Appl. Environ. Microbiol*. 56:1004–1011.
- Lupp, C., M.L. Robertson, M.E. Wickham, I. Sekirov, O.L. Champion, E.C. Gaynor, and B.B. Finlay. 2007. Host-mediated inflammation disrupts the intestinal microbiota and promotes the overgrowth of Enterobacteriaceae. *Cell Host Microbe*. 2:119–129. <https://doi.org/10.1016/j.chom.2007.06.010>
- Martinez, K.A. II, R.D. Kitko, J.P. Mershon, H.E. Adcox, K.A. Malek, M.B. Berken, and J.L. Slonczewski. 2012. Cytoplasmic pH response to acid stress in individual cells of Escherichia coli and Bacillus subtilis observed by fluorescence ratio imaging microscopy. *Appl. Environ. Microbiol*. 78:3706–3714. <https://doi.org/10.1128/AEM.00354-12>
- McMurdie, P.J., and S. Holmes. 2013. phyloseq: an R package for reproducible interactive analysis and graphics of microbiome census data. *PLoS One*. 8:e61217. <https://doi.org/10.1371/journal.pone.0061217>
- Ng, K.M., J.A. Ferreyra, S.K. Higginbottom, J.B. Lynch, P.C. Kashyap, S. Gopinath, N. Naidu, B. Choudhury, B.C. Weimer, D.M. Monack, and J.L. Sonnenburg. 2013. Microbiota-liberated host sugars facilitate post-antibiotic expansion of enteric pathogens. *Nature*. 502:96–99. <https://doi.org/10.1038/nature12503>
- O'Loughlin, J.L., D.R. Samuelson, A.G. Braundmeier-Fleming, B.A. White, G.J. Halderson, J.B. Stone, J.J. Lessmann, T.P. Eucker, and M.E. Konkel. 2015. The Intestinal Microbiota Influences Campylobacter jejuni Colonization and Extraintestinal Dissemination in Mice. *Appl. Environ. Microbiol*. 81:4642–4650. <https://doi.org/10.1128/AEM.00281-15>
- Rea, M.C., C.S. Sit, E. Clayton, P.M. O'Connor, R.M. Whittall, J. Zheng, J.C. Vederas, R.P. Ross, and C. Hill. 2010. Thuricin CD, a posttranslationally modified bacteriocin with a narrow spectrum of activity against Clostridium difficile. *Proc. Natl. Acad. Sci. USA*. 107:9352–9357. <https://doi.org/10.1073/pnas.0913554107>
- Rivera-Chávez, F., L.F. Zhang, F. Faber, C.A. Lopez, M.X. Byndloss, E.E. Olson, G. Xu, E.M. Velazquez, C.B. Lebrilla, S.E. Winter, and A.J. Bäumlner. 2016. Depletion of Butyrate-Producing Clostridia from the Gut Microbiota Drives an Aerobic Luminal Expansion of Salmonella. *Cell Host Microbe*. 19:443–454. <https://doi.org/10.1016/j.chom.2016.03.004>
- Roe, A.J., D. McLaggan, I. Davidson, C. O'Byrne, and I.R. Booth. 1998. Perturbation of anion balance during inhibition of growth of Escherichia coli by weak acids. *J. Bacteriol*. 180:767–772.
- Russell, A.B., S.B. Peterson, and J.D. Mougous. 2014. Type VI secretion system effectors: poisons with a purpose. *Nat. Rev. Microbiol*. 12:137–148. <https://doi.org/10.1038/nrmicro3185>
- Salmond, C.V., R.G. Kroll, and I.R. Booth. 1984. The effect of food preservatives on pH homeostasis in Escherichia coli. *J. Gen. Microbiol*. 130:2845–2850.
- Sonnenburg, E.D., and J.L. Sonnenburg. 2014. Starving our microbial self: the deleterious consequences of a diet deficient in microbiota-accessible carbohydrates. *Cell Metab*. 20:779–786. <https://doi.org/10.1016/j.cmet.2014.07.003>
- Sorbara, M.T., and E.G. Pamer. 2018. Interbacterial mechanisms of colonization resistance and the strategies pathogens use to overcome them. *Mucosal Immunol*. <https://doi.org/10.1038/s41385-018-0053-0>
- Taur, Y., J.B. Xavier, L. Lipuma, C. Ubeda, J. Goldberg, A. Gouberne, Y.J. Lee, K.A. Dubin, N.D. Succi, A. Viale, et al. 2012. Intestinal domination and the risk of bacteremia in patients undergoing allogeneic hematopoietic stem cell transplantation. *Clin. Infect. Dis*. 55:905–914. <https://doi.org/10.1093/cid/cis580>
- Taur, Y., K. Coyte, J. Schluter, E. Robilotti, C. Figueroa, M. Gjonbalaj, E.R. Littmann, L. Ling, L. Miller, Y. Gyaltsen, et al. 2018. Reconstitution of the gut microbiota of antibiotic-treated patients by autologous fecal microbiota transplant. *Sci. Transl. Med*. 10:eaap9489. <https://doi.org/10.1126/scitranslmed.aap9489>
- Topping, D.L., and P.M. Clifton. 2001. Short-chain fatty acids and human colonic function: roles of resistant starch and nonstarch polysaccharides. *Physiol. Rev*. 81:1031–1064. <https://doi.org/10.1152/physrev.2001.81.3.1031>
- Truong, D.T., E.A. Franzosa, T.L. Tickle, M. Scholz, G. Weingart, E. Pasolli, A. Tett, C. Huttenhower, and N. Segata. 2015. MetaPhlan2 for enhanced metagenomic taxonomic profiling. *Nat. Methods*. 12:902–903. <https://doi.org/10.1038/nmeth.3589>
- van der Waaij, D., J.M. Berghuis-de Vries, and J.E.C. Lekkerkerk-van der Wees. 1971. Colonization resistance of the digestive tract in conventional and antibiotic-treated mice. *J. Hyg. (Lond.)*. 69:405–411. <https://doi.org/10.1017/S0022172400021653>
- Wilks, J.C., and J.L. Slonczewski. 2007. pH of the cytoplasm and periplasm of Escherichia coli: rapid measurement by green fluorescent protein fluorimetry. *J. Bacteriol*. 189:5601–5607. <https://doi.org/10.1128/JB.00615-07>
- Winter, S.E., M.G. Winter, M.N. Xavier, P. Thiennimitr, V. Poon, A.M. Keestra, R.C. Laughlin, G. Gomez, J. Wu, S.D. Lawhon, et al. 2013. Host-derived nitrate boosts growth of E. coli in the inflamed gut. *Science*. 339:708–711. <https://doi.org/10.1126/science.1232467>
- Xiong, H., R.A. Carter, I.M. Leiner, Y.W. Tang, L. Chen, B.N. Kreiswirth, and E.G. Pamer. 2015. Distinct Contributions of Neutrophils and CCR2+ Monocytes to Pulmonary Clearance of Different Klebsiella pneumoniae Strains. *Infect. Immun*. 83:3418–3427. <https://doi.org/10.1128/IAI.00678-15>